Coordination Chemistry Reviews, 125 (1993) 283–292

Electronic coupling between remote metal centers in cyano-bridged polynuclear complexes.

F. Scandola, R. Argazzi, C. A. Bignozzi, C. Chiorboli, M. T. Indelli, and M. A. Rampi

Department of Chemistry, University of Ferrara, CNR Research Center on Photoreactivity and Catalysis, 44100 Ferrara, Italy

Abstract

Several cyanide-bridged polynuclear complexes have been synthesized in the context of intramolecular energy and electron transfer studies. A valence-localized description is generally appropriate for such complexes. Within such a localized picture, however, the cyanide bridge is found to provide a remarkable degree of metal-metal electronic coupling. This conclusion can be drawn from a variety of experimental results. Specific attention is devoted here to the spectroscopic observation of appreciable second-order interactions between *remote* (i.e., non directly bridged) sites in a polynuclear complex.

1. INTRODUCTION

Cyanide is an ambidentate ligand capable of binding simultaneously (*bridging*) two metal centers [1]. The most outstanding and long-known example of such type of binding mode is represented by mixed-valence solid materials of the Prussian Blue type. The binding properties of the two ends of cyanide are quite different. C-bonded cyanide behaves as a typical strong-field ligand, with good π-acceptor properties (probably related to the high π^* amplitude at C), and affinity for relatively electron-rich metals. On the other hand, N-bonded cyanide behaves more like a medium-field, mainly σ-donor, ligand, with affinity for relatively electron-poor metals. A clear example of this asymmetric behavior is the polymeric structure of Prussian Blue, where cyanide is C-bonded to low-spin Fe(II) and N-bonded to high-spin Fe(III).

Although polymeric cyano-bridged materials of such type have been known for a long time, discrete cyano-bridged complexes of well-defined nuclearity (e.g., binuclear and trinuclear complexes) have been synthesized and isolated only recently [2]. Detailed electrochemical, spectroscopic, and photophysical studies have been carried out on such molecular species, leading to the conclusion that a valence-localized description is generally appropriate for cyano-bridged polynuclear complexes [2,3]. Within such a localized picture, however, the cyanide bridge is found to provide a substantial amount of metal-metal electronic coupling in the polynuclear complex. Evidence for such coupling can be obtained from a variety of experimental results, including (i) intercomponent perturbation

0010-8545/93/$24.00

of electrochemical properties [4-9], (ii) intercomponent perturbation of UV/vis spectroscopic properties [4,5,7-9] , (iii) presence of intense intervalence transfer transitions in mixed-valence complexes [4,5,9], (iv) presence of related transitions in excited-state UV/vis spectra [10,11], (v) intercomponent perturbation of ligand stretching frequencies in excited-state IR spectra [12], (vi) second-order interactions between remote sites [4,5,7,9].

Point (vi) is related to the fact that, in a cyano-bridged polynuclear complex, appreciable electronic coupling can take place even between metal centers which are not directly bound via a cyanide bridge. For example in some trinuclear complexes of the type

$$\mathrm{M_1\text{-}(CN)\text{-}M_2\text{-}(CN)\text{-}M_3}$$

where M_1, M_2, and M_3 represent metal centers, spectroscopic evidence for appreciable electronic coupling between M_1 and M_3 has been obtained. This problem will be discussed in some detail in this article.

2. REMOTE INTERVALENCE TRANSFER

The example to be discussed belongs to a series of bi- and trinuclear complexes of general formulae $[\mathrm{X(NH_3)_4Ru\text{-}NC\text{-}Ru(bpy)_2\text{-}CN}]^{n+}$ and $[\mathrm{X(NH_3)_4Ru\text{-}NC\text{-}Ru(bpy)_2\text{-}CN\text{-}Ru(NH_3)_4Y}]^{m+}$ (X = $\mathrm{NH_3}$, py; Y = $\mathrm{NH_3}$, py; n = 2,3; m = 4-6) [3-5]. The possible combinations of (i) X and Y ancillary ligands and (ii) oxidation states of the $[\mathrm{\text{-}Ru(NH_3)_4X}]^{3+/2+}$ and/or $[\mathrm{\text{-}Ru(NH_3)_4Y}]^{3+/2+}$ subunits give rise to a large number of complexes within this series. Let us consider, as a prototypal case within this series, the species shown in Fig. 1. In this species, several electronic states are relevant, with the following one-electron configurations ($^{-\cdot}$ represents the radical anion of the ligand):

(0) ground state:
$$[\mathrm{py(NH_3)_4Ru^{II}\text{-}NC\text{-}Ru^{II}(bpy)_2\text{-}CN\text{-}Ru^{III}(NH_3)_5}]^{5+}$$

(1) Ru → bpy MLCT:
$$[\mathrm{py(NH_3)_4Ru^{II}\text{-}NC\text{-}Ru^{III}(bpy^{-\cdot})(bpy)\text{-}CN\text{-}Ru^{III}(NH_3)_5}]^{5+}$$

(2) Ru → py MLCT:
$$[\mathrm{(py^{-\cdot})(NH_3)_4Ru^{III}\text{-}NC\text{-}Ru^{II}(bpy)_2\text{-}CN\text{-}Ru^{III}(NH_3)_5}]^{5+}$$

(3) Ru → bpy remote MLCT:
$$[\mathrm{py(NH_3)_4Ru^{III}\text{-}NC\text{-}Ru^{II}(bpy^{-\cdot})(bpy)\text{-}CN\text{-}Ru^{III}(NH_3)_5}]^{5+}$$

(4) Ru → Ru IT:
$$[\mathrm{py(NH_3)_4Ru^{II}\text{-}NC\text{-}Ru^{III}(bpy)_2\text{-}CN\text{-}Ru^{II}(NH_3)_5}]^{5+}$$

(5) Ru → Ru remote IT:
$$[\mathrm{py(NH_3)_4Ru^{III}\text{-}NC\text{-}Ru^{II}(bpy)_2\text{-}CN\text{-}Ru^{II}(NH_3)_5}]^{5+}$$

Of these excited states, types 1 and 2 would be present in the isolated components as well, but 3-5 are new states of intercomponent charge transfer type, characteristic of the polynuclear species as such. Transitions corresponding to the various types of excited states can be easily identified in the absorption spectrum of this complex. The resolution of the absorption spectrum of the complex into various types of transitions is shown in Fig. 2. By selective oxidation or reduction of the various sites in the molecule, very clear spectral changes take place, making the attribution of the various types of transitions straightforward [3,4].

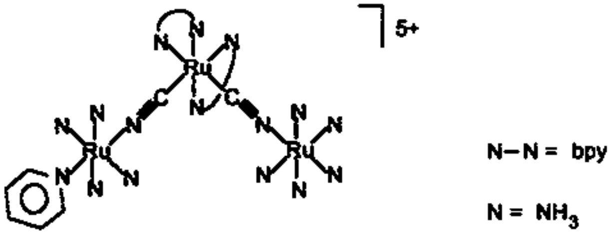

Fig. 1. Schematic structure of the $[py(NH_3)_4Ru^{II}\text{-}NC\text{-}Ru^{II}(bpy)_2\text{-}CN\text{-}Ru^{III}(NH_3)_5]^{5+}$ trinuclear complex.

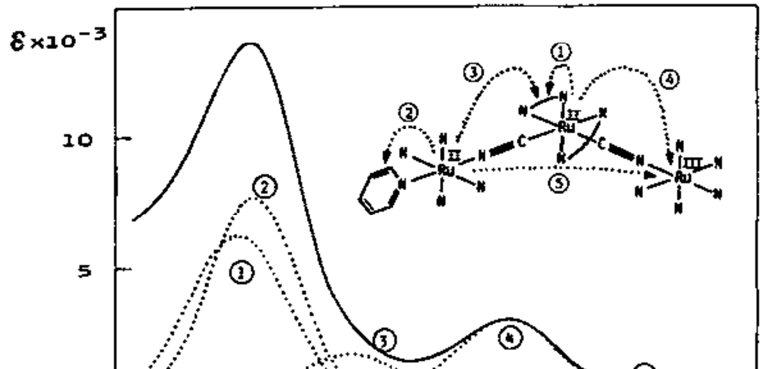

Fig. 2. Resolution of the absorption spectrum of $[py(NH_3)_4Ru\text{-}NC\text{-}Ru(bpy)_2\text{-}CN\text{-}Ru(NH_3)_5]^{5+}$ into various types of charge transfer transitions.

The various types of optical electron transfer transitions can be analyzed in terms of Hush model, which relates band energy, intensity and halfwidth with thermodynamic energy gradient, ΔE, center-to-center electronic coupling, H_{AB}^{el}, and reorganizational energy λ [13-15]. The analysis of the intervalence transfer transition taking place across the cyanide bridge (transition of type 4) provides the following values: $H_{AB}^{el} \approx 1800\ cm^{-1}$, $\lambda \approx 8700\ cm^{-1}$, $\Delta E \approx 5600\ cm^{-1}$. The substantial coupling provided by cyanide is apparent, but the degree of electron delocalization between the two metal centers, $\alpha^2 = (H_{AB}^{el})^2/(\lambda + \Delta E)^2 = 0.02$, is sufficiently small to warrant a localized description of this trinuclear complex.

Of particular interest from the point of view of the present discussion is the direct observation of *remote* IT (type 5). Since intensity is primarily related to electronic coupling [13-15], this observation proves that sizable electronic coupling between non-directly-bridged, "remote", redox sites is present in these system. An analysis of the remote IT transition according to Hush model [13-15] yields $H_{AB}^{el} \approx 300\ cm^{-1}$ between the terminal metal centers of this trinuclear complex. The experimental result is very clear, but the origin of such a remarkable electronic coupling is puzzling. As a matter of fact, a *through-space* mechanism, i.e., direct orbital overlap between two metals lying ≈ 7 Å apart, seems to be unplausible for an electronic coupling of this size. Thus, some *through-bond* mechanism is likely to be involved in the interaction between remote metal centers.

Three related trinuclear complexes (Fig 3), with the same distribution of

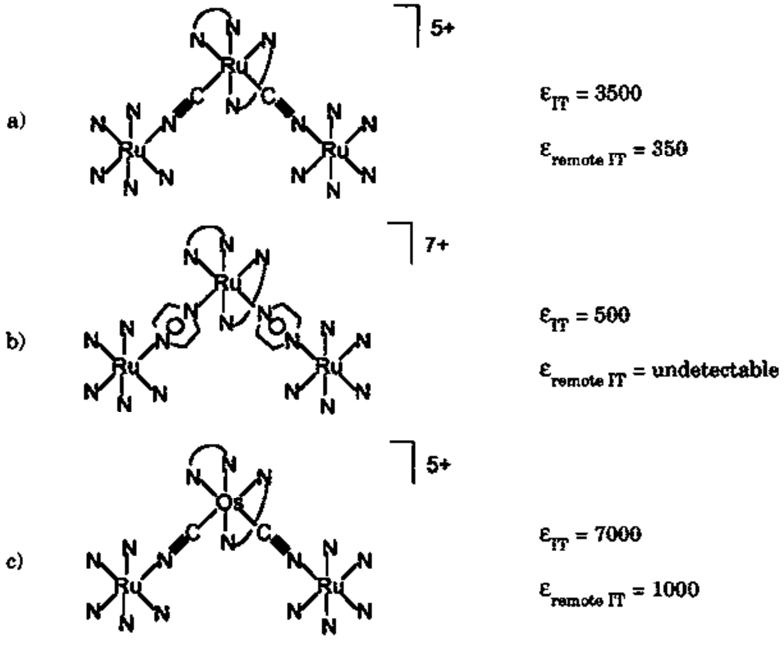

Fig 3. Schematic structures of trinuclear complexes related to the complex of Fig 1 (same symbols and abbreviations), and molar absorptivities of the IT and "remote" IT absorption bands in their spectra.

oxidation states between the metal centers, have been investigated by the authors (Figs 3a [4] and 3c [16]) and by Meyer and coworkers (Fig. 3b [17]). It is interesting to note (Fig 3) that the intensity of remote IT changes widely among these complexes, in a way that is hardly related with expected metal-metal bond distances, but seems to depend strongly on the groups (bridging ligands and metal) interposed between the two remote metals. This again points towards some through-bond rather than through-space mechanism.

3. SUPEREXCHANGE

One of the simplest models to deal with through-bond interactions in covalently bonded supramolecular systems is that of *superexchange* [18-23]. Consider an A-L-B system in which the redox orbitals of the A and B molecular components do not overlap appreciably with each other, due to the large A-B distance. They do overlap, however, with appropriate orbitals (HOMO and LUMO) of the L bridge, resulting in an indirect, through-bridge, mixing. In terms of electron configurations, this amounts to consider that the initial and final states of the electron transfer process are coupled together *via* interaction with high-energy states involving electron transfer from or to the connector (Fig. 4). The two "intermediate" states can be conveniently called *electron-transfer* (A^+-L^--B) and *hole-transfer* (A-L^+-B^-) states. It is important to realize that there is nothing such as a real electron (or hole) hopping from A to L to B in this mechanism: the electron transfer occurs in a single step from A to B. The electron- and hole-transfer configurations help to propagate the interaction, but they usually occur at high energies and the corresponding states are never populated during the process. These states are thus often designated as "virtual states".

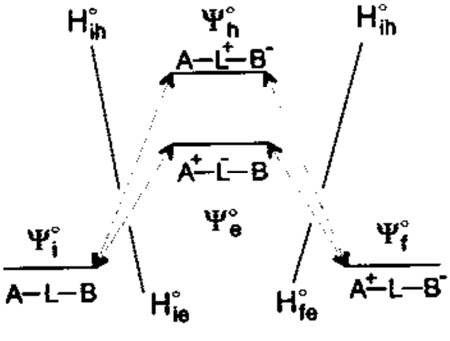

Fig. 4. Energy level diagram illustrating superexchange interaction between a donor A and an acceptor B through a bridging group L. The figure represents zero-order states corresponding to pure, localized electronic configurations: Ψ°_i and Ψ°_f are the initial and final states of an electron transfer process, while Ψ°_e and Ψ°_h are electron- and hole-transfer states involving the bridge. For the other symbols, see text.

A more quantitative picture of the factors that affect the magnitude of the superexchange interaction can be obtained from perturbation theory. Let us label with *i*, *f*, *e*, and *h* the initial, final, electron- and hole-transfer states, respectively.

Let us also use the *o* superscript (as, for example, in Ψ°) to indicate wavefunctions, matrix elements, and energy differences relating to zero-order states, i.e, states that correspond to pure, localized electronic configurations. In the limit of small electron delocalization, the true initial and final states of the electron transfer process are given by an appropriate admixture of the corresponding zero-order states (eqs 1,2). According to second-order perturbation

$$\Psi_i \approx \Psi^\circ_i + \alpha\,\Psi^\circ_f \tag{1}$$

$$\Psi_f \approx \Psi^\circ_f - \alpha\,\Psi^\circ_i \tag{2}$$

theory, the initial wavefunction is given by eq 3, where the H° and ΔE° terms are the matrix elements and the energy differences, respectively, between the various

$$\Psi_i = \Psi^\circ_i + \frac{H^\circ_{if}}{\Delta E^\circ_{if}}\,\Psi^\circ_f + \left[\frac{H^\circ_{ie}\,H^\circ_{fe}}{\Delta E^\circ_{ie}\ \Delta E^\circ_{if}} + \frac{H^\circ_{ih}\,H^\circ_{fh}}{\Delta E^\circ_{ih}\ \Delta E^\circ_{if}} + \frac{H^\circ_{ii}\,H^\circ_{if}}{(\Delta E^\circ_{if})^2}\right]\Psi^\circ_f \tag{3}$$

zero-order states. Since the first-order perturbation matrix element H°_{if} is equal to zero because of the negligible direct orbital overlap between A and B, the mixing coefficient is given by eq 4. If we define the effective electronic coupling

$$\alpha = \frac{H^\circ_{ie}\,H^\circ_{fe}}{\Delta E^\circ_{ie}\ \Delta E^\circ_{if}} + \frac{H^\circ_{ih}\,H^\circ_{fh}}{\Delta E^\circ_{ih}\ \Delta E^\circ_{if}} \tag{4}$$

between the initial and final states, H_{AB}, from $\alpha = H_{AB}/\Delta E_{if}$, and consider $\Delta E_{if} \approx \Delta E_{if}^\circ$, then

$$H_{AB} \approx \frac{H^\circ_{ie}\,H^\circ_{fe}}{\Delta E^\circ_{ie}} + \frac{H^\circ_{ih}\,H^\circ_{fh}}{\Delta E^\circ_{ih}} \tag{5}$$

In eq 5, the energy differences ΔE°_{ie} and ΔE°_{ih} are to be taken at the geometry of the crossing point.

In the common case where L is a simple bridging group (e.g., and organic spacer in organic donor-acceptor dyads, or a bridging ligand between two metal centers), the electron- and hole-transfer states lie at very high energies ("virtual" states) and it is difficult to have reliable values for the quantities (energies, intermediate couplings) involved, according to (5), in the calculation of the electronic coupling. At least formally, the trinuclear complexes discussed in the previous section can be considered as A-L-B systems in which the two terminal metal centers play the role of A and B, while the central metal fragment (possibly together with the bridging ligands) constitutes the L "bridge". In this case, the electron- and hole-transfer states involving the bridge may occur at low energy and be spectroscopically observable. For instance, in the case of Fig. 2, the electron- transfer state is the remote MLCT state (corresponding transition, 3) and the hole-transfer state is the IT state (corresponding transition, 4). The analysis of these spectroscopic transitions according to Hush model [13-15] (subject to some assumptions [24]) yields the appropriate ΔE and H values, to be used in eq 5. When this is done for the case of Fig. 2, the following values are obtained $H^{\circ}_{ie} = H^{\circ}_{fe} = 1500$ cm^{-1}, $H^{\circ}_{ih} = H^{\circ}_{fh} = 1900$ cm^{-1}, $\Delta E^{\circ}_{ie} = 16000$ cm^{-1}, $\Delta E^{\circ}_{ih} = 9900$ cm^{-1}. By substituting these values in eq 5, an end-to-end superexchange coupling of 500 cm^{-1} is calculated. This can be compared with the actual coupling of 300 cm^{-1}, obtained from the spectroscopic parameters of the end-to-end IT transition (transition 5 in Fig 2). Given the approximations involved, the agreement is satisfactory. Thus, electronic coupling between remote metal centers in these trinuclear complexes occurs mainly through-bond, and the mechanism can be conveniently represented, at least qualitatively, by superexchange.

According to eq 5, good "conducting" bridges (i.e., bridges with good ability to produce superexchange coupling) must (i) possess low-lying charge (electron- or hole-) transfer states and (ii) be efficiently coupled to the terminal units. In the case of the complex "bridge" present in the system of Fig 2, these features are brought about by (i) the redox properties of central metal and its non-bridging ligands and (ii) the electronic properties (short distance, efficient π-bonding) of the bridging cyanides.

It is instructive to compare, from this point of view, the complex of Figs 1 and 2 with those in Fig 3. It is seen that there is a *correlation* between the intensity of the IT band between adjacent metal centers and that of the remote IT band. As a matter of fact, given the relationship between electronic coupling and band intensity [13-15], eq 5 actually predicts that the remote IT band "steals" intensity from nearby charge transfer bands (IT and remote MLCT) involving the central metal-containing bridge. Since the reasons for the changes in intensity of the IT band along this series of complexes can be reasonably explained in terms of bonding arguments, including the nature of the bridging ligands and the metal, a basis for the rationalization of the observed remote couplings is available. For example, in the comparison between the complexes of Figs 3a and 3b, cyanide provides better coupling than pyrazine between adjacent metal centers (as witnessed by the intensity of the IT transition), and this results in a stronger remote coupling between the two terminal units. The difference between the complexes of Figs 3a and 3c can be rationalized in terms of the greater orbital size and tendency to π back bonding of Os relative to Ru.

4. SPLITTING OF DEGENERATE IT TRANSITIONS

The example discussed here belongs to a series of polychromophoric complexes designed for to intercomponent energy transfer studies [7]. These are the binuclear and trinuclear cyano-bridged complexes

$$[\mathrm{NC\text{-}Ru^{II}(bpy)_2\text{-}CN\text{-}Ru^{III}(bpy)_2\text{-}CN}]^{2+}$$

and

$$[\mathrm{NC\text{-}Ru^{II}(bpy)_2\text{-}CN\text{-}Ru^{III}(bpy)_2\text{-}NC\text{-}Ru^{II}(bpy)_2\text{-}CN}]^{3+}$$

In these complexes, the only structural differences between the various Ru-centered units are made by the cyanide ligands (bridging vs. terminal, C- bonded vs. N-bonded). In the mixed-valence forms depicted above, these differences

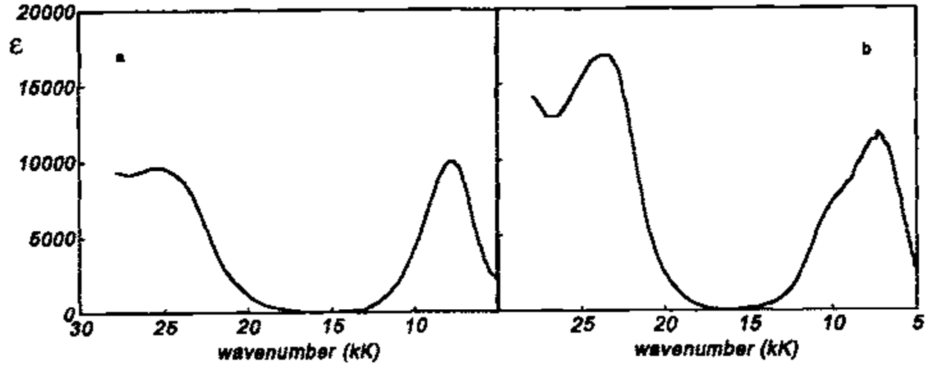

Fig. 5. Spectra of the mixed-valence complexes $[NC-Ru^{II}(bpy)_2-CN-Ru^{III}(bpy)_2-CN]^{2+}$ (a) and $[NC-Ru^{II}(bpy)_2-CN-Ru^{III}(bpy)_2-NC-Ru^{II}(bpy)_2-CN]^{3+}$ (b).

determine the distribution of oxidation states between the metal centers. The vis/near-IR spectra of these complexes are shown in Fig. 5.

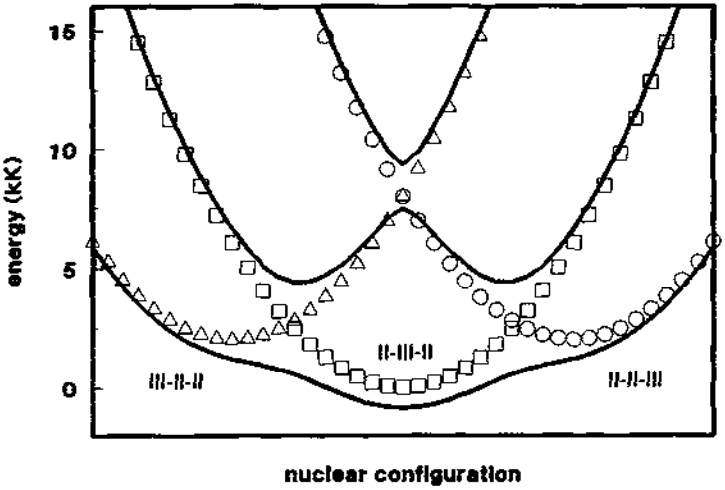

Fig. 6. Schematic representation of non-interacting (dotted curves) and interacting (continuous lines) energy surfaces for a symmetrical trinuclear mixed-valence complex such as $[NC-Ru^{II}(bpy)_2-CN-Ru^{III}(bpy)_2-NC-Ru^{II}(bpy)_2-CN]^{3+}$. The interacting curves are calculated assuming electronic couplings of 2000 cm^{-1} between adjacent metal centers, and 1000 cm^{-1} between terminal ones.

Besides the usual MLCT bands in the visible, these spectra show clear Ru(II) → Ru(III) intervalence bands in the near-IR region. Analysis of the intervalence transfer band of the binuclear complex according to Hush theory [13-15] yields

$H_{AB}^{el} = 2000\ cm^{-1}$, $\lambda = 5700\ cm^{-1}$, $\Delta E = 2000\ cm^{-1}$, and $\alpha^2 = (H_{AB}^{el})^2/(\lambda + \Delta E)^2 = 0.07$, indicating again a substantially valence-localized structure with, however, considerable intercomponent interaction. A remarkable observation is that in this case, as well as in other related bi- and trinuclear systems [9], the intervalence transfer transition for the trinuclear complex is not simply twice as intense as that of the binuclear one (as would be expected on the basis of its degeneracy) but rather seems to be split into two transitions of comparable intensity and slightly different energy. A likely explanation of this fact brings again into focus a non-negligible electronic coupling between remote sites. Fig. 6 shows a schematic representation of this situation in terms of (i) zero-order non-interacting curves for ground state and the two "degenerate" intervalence transfer states, and (ii) first order curves allowing for the intercomponent interactions. The coupling between remote centers required to reproduce (at the avoided crossing between the two zero-order intervalence transfer states) the observed spectral splitting is compatible with the expectations of a model similar with that of Section 3 (Fig. 4), in which the Ψ^o_i and Ψ^o_f are now degenerate excited states and Ψ^o_h is the ground state.

5. CONCLUSIONS

In cyano-bridged polynuclear ruthenium complexes, thanks to the large electronic coupling provided by bridging cyanide between adjacent units, electronic interaction can extend appreciably over at least three metal centers. Some spectroscopic consequences of electronic coupling between remote metal centers in trinuclear complexes have been discussed.

6. ACKNOWLEDGMENT

We wish to express our deep gratitude to Vittorio Carassiti, who showed us the way into the wonderful land of photochemistry. It has been a privilege to work with him for all these years, taking advantage of his constant advice and encouragement.

7. REFERENCES

1 Shriver, D. F. *Struct. Bonding* **1966**, *1*, 32.

2 Scandola, F.; Bignozzi, C. A.; Indelli, M. T. In *Photosensitization and Photocatalysis using Inorganic and Organometallic Compounds*; Kalyanasundaram, K.; Grätzel, M., Eds.: Kluwer Academic Publishers: Dordrecht, 1993.

3 Schoonover, J. R.; Timpson, C. S.; Meyer, T. J.; Bignozzi, C. A. *Inorg. Chem.* **1992**, *31*, 3185.

4 (a) Bignozzi, C. A.; Roffia, S.; Scandola, F. *J. Am. Chem. Soc.* **1985**, *107*, 1644. (b) Bignozzi, C. A., Paradisi, C., Roffia, S., and Scandola, F. *Inorg. Chem.* **1988**, *27*, 408. (c) Roffia, S.; Casadei, R.; Paolucci, F.; Paradisi, C.; Bignozzi, C. A.; Scandola, F. *J. Electroanal. Chem.* **1991**, *302*, 157.

5 Roffia, S.; Paradisi, C.; Bignozzi, C. A. *J. Electroanal. Chem.* **1986**, *200*, 10.

6 Bignozzi, C. A.; Indelli, M. T.; Scandola, F. *J. Am. Chem. Soc.* **1989**, *111*, 5192.
7 Bignozzi, C. A.; Roffia, S.; Chiorboli, C. ; Davila, J.; Indelli, M. T.; Scandola, F. *Inorg. Chem.* **1989**, *28*, 4350.
8 Roffia, S.; Ciano, M. *J. Electroanal. Chem.* **1977**, *77*, 349.
9 Bignozzi, C. A.; Argazzi, R.; Schoonover, J. R.; Gordon, K. C.; Dyer, R. B.; Scandola, F. *Inorg. Chem.* **1992**, *31*, 5260.
10 Bignozzi, C. A.; Argazzi, R.; Chiorboli, C.; Roffia, S.; Scandola, F. *Coord. Chem. Rev.* **1991**, *111*, 261.
11 Bignozzi, C. A.; Argazzi, R.; Chiorboli, C.; Scandola, F.; Schoonover, J. R.; Meyer T. J. manuscript in preparation.
12 Gordon, K. C.; Dyer, R. B.; Schoonover, J. R.; Meyer, T. J.; Argazzi, R.; Bignozzi, C. A. *J. Phys. Chem.*, in press.
13 Creutz, C. *Prog. Inorg. Chem.* **1983**, *30*, 1.
14 Hush, N. S. *Prog. Inorg. Chem.* **1967**, *8*, 391.
15 Balzani, V. ; Scandola, F.; *Supramolecular Photochemistry*; Horwood: Chichester, 1991; Chapter 3.
16 Bignozzi, C. A., unpublished results.
17 Powers, M. J.; Callahan, R. W.; Salmon, D. J.; Meyer, T. J. *Inorg. Chem.* **1976**, *15*, 894.
18 Halpern, J.; Orgel, L. E. *Disc. Faraday Soc.* **1960**, *29*, 32.
19 McConnell H. M. *J. Chem. Phys.* **1961**, *35*, 508.
20 Day, P. *Comments Inorg. Chem.* **1981**, *1*, 155.
21 Miller, J. R.; Beitz, J. V. *J. Chem. Phys.* **1981**, *74*, 6746.
22 Richardson, D. E.; Taube, H. *J. Am. Chem. Soc.* **1983**, *105*, 40.
23 Wasielewski, M. R. In *Photoinduced electron transfer*; Fox, M. A.; Chanon, M., Eds.: Elsevier, 1988. Part A, p. 161
24 These numbers are obtained by assuming: (i) same parabolic curves for initial, final, and "intermediate" states; (ii) minima of "intermediate" states halfway between those of initial and final states along the nuclear reorganizational coordinate.